Ab initio and DFT investigations on Acetoacetanilidimine Derivative

Ab initio……

C.Chelladurai[1]
Assistant Professor, Department of Chemistry, Angle College of Engineering & Technology, Tiruppur- 641 665, INDIA

Dr. V.D. Nadhiya[2]
Assistant Professor, Department of Physics, Kongunadu Arts and Science College (Autonomous), Coimbatore-641029, INDIA

Dr. N. Neelakandeswari[3]
Associate Professor, Department of Chemistry, Sri Ramakrishna Engineering College (Autonomous), Coimbatore-641 022, INDIA

Dr. A. Manimaran [4]*+
Assistant Professor, Department of Chemistry, Kongunadu Arts and Science College (Autonomous), Coimbatore-641029, INDIA.

Abstract : *Ab* initio and DFT investigations on acetoacetanilidimine derivative viz., 3-((2-((2-hydroxy-3-methoxybenzylidene)amino)phenyl)imino)-N-phenylbutanamide by using B3LYP/6-311G(d,p) level of theory. The delocalization and mobility of electrons in the title compound was obtained from the geometry optimization, vibrational frequencies (IR), electronic transition, TD-DFTand NMR shielding tensors (^{13}C and ^{1}H). The chemical reactivity of the compound is studied by the simulation of molecular electrostatic potential surface, PES and FMO with molecular energy level diagram. The fundamental vibrational modes and wave numbers of acetoacetanilidimine derivative are characterized theoretically based on potential energy distribution. In addition to that, Mulliken Charges, APT charges and hyperpolarizability (β_{tot}) as NLO studies were also calculated.

KEYWORDS: Acetoacetanilidimine; MEP; TD-DFT; NMR shielding tensors; FMOs; hyperpolarizability.

I. INTRODUCTION

Schiff base compounds are most important class of organic compounds which have attracted considerable attention due to their wide applications such as organic dyes, catalyst and schiff base compounds exhibit a broad range of biological activities [1-4]. They are used for industrial purpose and have variety of biological activities antidepressants, antimicrobial, antitumor, antiphlogogistic, nematocide, and other medicinal agents have been reported based on these compounds [5-11]. The important structural properties of acetoacetanilidimine derivatives play a major role for the development of new drug and NLO applications [12-14]. The investigation of influence of substitutions in the derivatives can be helpful in future design of complex with tunable properties [15-18]. In order to investigate the reactive sites of the molecule and electrophilic and nucleophilic attack sites of the molecule, the molecular electrostatic potential map was established by using B3LYP/6-31G(d,p) method. The energy gap between HOMO and LUMO is a critical parameter to determine molecular electrical transport properties [19]. Calculations of partial atomic charges are useful factor to predict the dipole moments, electronic structures, polarizabilities and chemical reactivities of the molecules [20, 21] and also to understand the quantum mechanical relationship between the types of substituent such as donor and acceptor and NLO properties, we explore the theoretical studies ON acetoacetanilidimine derivativeviz.,3-((2-((2-hydroxy-3-methoxybenzylidene)amino)phenyl)imino)-N-phenylbutanamide **(AAVA)**.

II. THEORETICAL INVESTIGATION

DFT Calculations

The schiff base compound derived from acetoacetanilidimine [14](Scheme 1) have active anilide group which is most polarizable, the DFT study is vitalto determine the structural parameters in accuracy with B3LYP/6-311G(d,p) level theory and quantum mechanical investigations have been computed with the GAUSSIAN 09W program package [22-27]. The program used to

optimize structures, and calculate PES, vibrational frequencies (IR), electronic transition, TD-DFT and gauge-including atomic orbitals (GIAOs) to calculate NMR shielding tensors (^{13}C and ^{1}H) [28-31].

The Mulliken Charges, APT charges, the energies of the frontier molecular orbitals (HOMO/LUMO) with molecular energy level diagram, electrostatic potential surface and Laplacian electron density analysis and molecular first static hyperpolarizability (β_{tot}) was also computed [32-36].

The GaussView6.0.16 visualization programme [35] and Chemcraft version 1.8 have been employed to generate the Laplacian electron density maps, HOMO-LUMO and ESP contour surfaces.

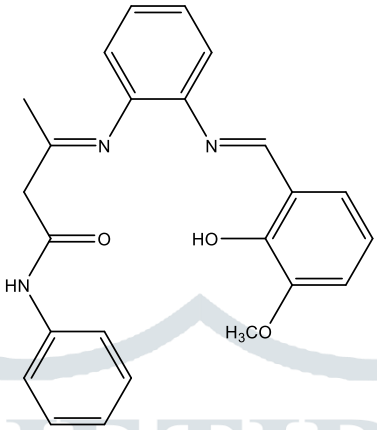

3-((2-((2-hydroxy-3-methoxybenzylidene)amino)phenyl)imino)-*N*-phenylbutanamide

Scheme 1. Keto form of AAVA

III. RESULTS AND DISCUSSION

III. 1. Geometry Optimization

The geometry optimization without symmetry constraints of C-C and C-H bond lengths and bond angles by -H and $–CH_3$ substituent at diamine moiety was carried out and the optimized structure of the AAVA and it potential energy surface diagram (PES) with numbering the atoms are shown in Fig. 1 and Fig. 2. The optimized bond lengths, bond angles and dihedral angles were obtained using B3LYP with 6-311G(d,p) level theory and given in Table 1. The potential energy surface of reported compounds has been carried out to find existence of conical intersection between the ground and first excited state, however, the DFT based B3LYP/6-311G (d,p) level of computations were not able to predict any imaginary frequencies implying that the stationary point is located at the global minimum of the potential energy hyper-surface (Fig. 2). The calculated optimized electronic energy of AAVA is-1318.65 Hartree with the Zero point energy correction 0.4245 Hartree, respectively. Based on the computed zero-point vibrational energy of the AAVA, the molecular stability is confirmed. The analytical and thermodynamical parameters of reported compound with 298.150 K at 1.000 atm pressure reported in and the bond distances and bond angles in Table 2.

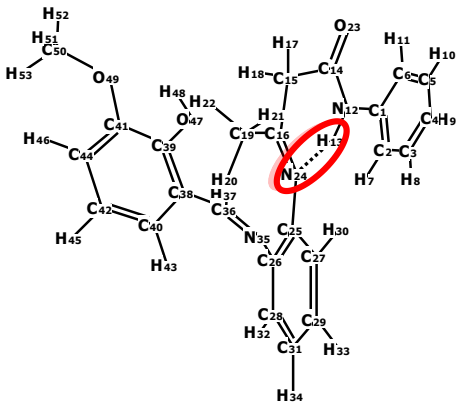

Scheme 2.Optimized structure AAVA with intermolecular hydrogen bonding

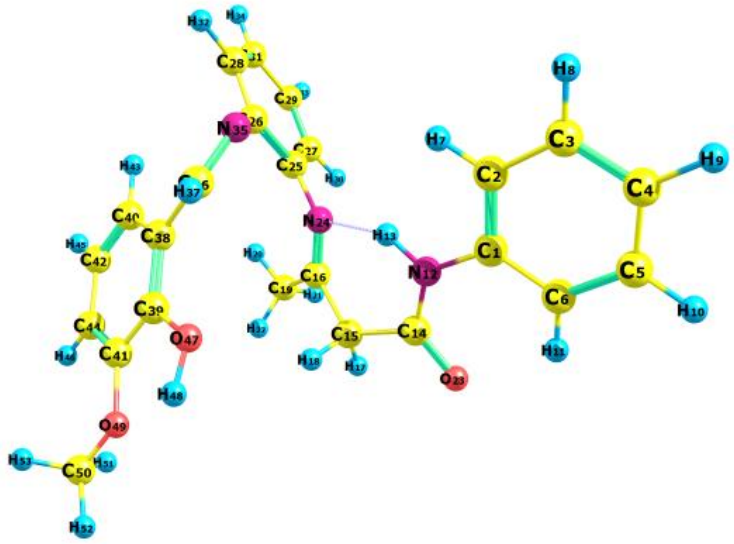

Fig. 1:Optimized structure of AAVA with numbering of atoms

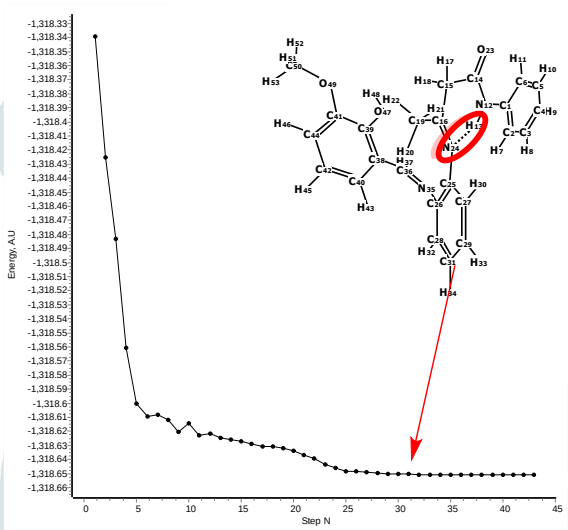

Fig. 2: PES diagram of AAVA

Table 1.Optimized Geometrical bond lengths of AAVA

S.No.	Bond Length		Bond Angle	
	Bond atoms	Bond Length (Å)	Bond atoms	Bond Angle (Å)
1.	H(53)-C(50)	1.095	O(49)-C(50)-H(51)	111.105
2.	H(52)-C(50)	1.088	O(49)-C(50)-H(52)	105.985
3.	H(51)-C(50)	1.095	O(49)-C(50)-H(53)	111.111
4.	C(50)-O(49)	1.424	C(41)-O(49)-C(50)	118.576
5.	O(49)-C(41)	1.372	C(39)-O(47)-H(48)	107.456
6.	H(48)-O(47)	0.968	C(42)-C(44)-C(41)	119.360
7.	O(47)-C(39)	1.361	C(44)-C(42)-C(40)	120.598
8.	H(46)-C(44)	1.082	O(49)-C(41)-C(44)	126.463
9.	H(45)-C(42)	1.083	O(49)-C(41)-C(39)	113.353
10.	C(44)-C(42)	1.401	C(44)-C(41)-C(39)	120.184
11.	C(44)-C(41)	1.387	C(42)-C(40)-C(38)	120.761
12.	H(43)-C(40)	1.081	O(47)-C(39)-C(41)	119.553
13.	C(42)-C(40)	1.385	O(47)-C(39)-C(38)	119.818
14.	C(41)-C(39)	1.408	C(41)-C(39)-C(38)	120.604
15.	C(40)-C(38)	1.407	C(36)-C(38)-C(40)	123.061
16.	C(39)-C(38)	1.398	C(36)-C(38)-C(39)	118.304
17.	C(38)-C(36)	1.482	C(40)-C(38)-C(39)	118.486
18.	H(37)-C(36)	1.091	N(35)-C(36)-C(38)	129.857
19.	C(36)-N(35)	1.274	C(26)-N(35)-C(36)	124.509
20.	N(35)-C(26)	1.403	C(29)-C(31)-C(28)	119.927
21.	H(34)-C(31)	1.084	C(31)-C(29)-C(27)	119.728
22.	H(33)-C(29)	1.084	C(31)-C(28)-C(26)	121.018
23.	H(32)-C(28)	1.084	C(29)-C(27)-C(25)	121.182
24.	C(31)-C(29)	1.394	N(35)-C(26)-C(28)	119.387
25.	C(31)-C(28)	1.390	N(35)-C(26)-C(25)	121.077

26.	H(30)-C(27)	1.084	C(28)-C(26)-C(25)	119.164
27.	C(29)-C(27)	1.391	N(24)-C(25)-C(27)	122.621
28.	C(28)-C(26)	1.400	N(24)-C(25)-C(26)	117.997
29.	C(27)-C(25)	1.401	C(27)-C(25)-C(26)	118.933
30.	C(26)-C(25)	1.417	C(16)-N(24)-C(25)	125.443
31.	C(25)-N(24)	1.406	C(16)-C(19)-H(21)	110.152
32.	N(24)-C(16)	1.276	C(16)-C(19)-H(22)	109.472
33.	O(23)-C(14)	1.220	C(19)-C(16)-C(15)	114.424
34.	H(22)-C(19)	1.094	C(19)-C(16)-N(24)	126.296
35.	H(21)-C(19)	1.095	C(15)-C(16)-N(24)	119.159
36.	H(20)-C(19)	1.088	C(14)-C(15)-C(16)	121.778
37.	C(19)-C(16)	1.510	O(23)-C(14)-N(12)	125.862
38.	H(18)-C(15)	1.099	O(23)-C(14)-C(15)	118.734
39.	H(17)-C(15)	1.091	N(12)-C(14)-C(15)	115.321
40.	C(16)-C(15)	1.520	H(13)-N(12)-C(1)	117.087
41.	C(15)-C(14)	1.540	H(13)-N(12)-C(14)	113.911
42.	C(14)-N(12)	1.362	C(1)-N(12)-C(14)	128.838
43.	H(13)-N(12)	1.022	C(1)-C(6)-C(5)	119.428
44.	N(12)-C(1)	1.408	C(6)-C(5)-C(4)	121.266
45.	C(6)-C(1)	1.402	C(5)-C(4)-C(3)	119.136
46.	C(6)-C(5)	1.393	C(4)-C(3)-C(2)	120.372
47.	C(5)-C(4)	1.392	C(3)-C(2)-C(1)	120.425
48.	C(4)-C(3)	1.394	N(12)-C(1)-C(6)	123.683
49.	C(3)-C(2)	1.389	N(12)-C(1)-C(2)	116.943
50.	C(2)-C(1)	1.404	C(6)-C(1)-C(2)	119.373

Table 2:Analytical and thermochemistry of AAVA with 298.150 K at 1.000 atm pressure

Molecular formulae	$C_{24}H_{23}N_3O_3$
Electronic energy (Hartree)	-1318.65
Zero point energy correction (Hartree)	0.4245
Thermal correction to energy (Hartree)	0.4517
Thermal correction to enthalpy (Hartree)	0.4526
Thermal Energy (Kcal/mol)	283.436
Heat capacity (cal/mol. kelvin)	104.496
Entropy (cal/mol.kelvin)	188.752
Dipole moment (Debye)	8.2

The bond lengths between the diamine nitrogen and the aromatic ring, C36-N35, C16-N24 at 1.274Å, 1.276Å and C16-N24-C25, C26-N35-C36at 125Å,124Årespectively. The bond distance slightly increases for C12-C13 is due the influence of adjacent highly polar carbonyl group. With the electron donating methyl substituent on the diamine moiety, the symmetry of the ring is distorted, yielding ring angles smaller than 120 at C28-C26-C25 and slightly larger than 120 at the ortho and meta positions [15,37].

III.2. Mulliken electronegativity and APT Charges

The quantum chemical calculations are used to determine electronegativity of pure s, p and d states and atomic partial charges (APT) for the reported compound involves fitting the charges to electrostatic potentials (ESPs) computed with *abinitio* quantum mechanics at sampling points around the reported compounds(Fig. 3). Mulliken electronegativity (χ) can be computed as follows: $\chi=(I+A)/2$, where I is ionization energy ($I=-E_{HOMO}$) and A is electron affinity ($A=-E_{LUMO}$). Softness is measure of extent of chemical reactivity as $S=1/2\eta$ and harness is measured as $\eta=(I-A)/2$. The electrophilicity index $\omega=(-\chi^2/2\eta)$ is a measure of energy lowering due to maximum electron flow between donor and acceptor [38,39]. The results indicate that the hetero atoms with high

negative charges, that is, nitrogen and oxygen atoms could act as electron donors and coordinate with metals [20]. The values of elecltronegativity, hardness, softness, electrophilicity index, energy gap are presented in Table 3.

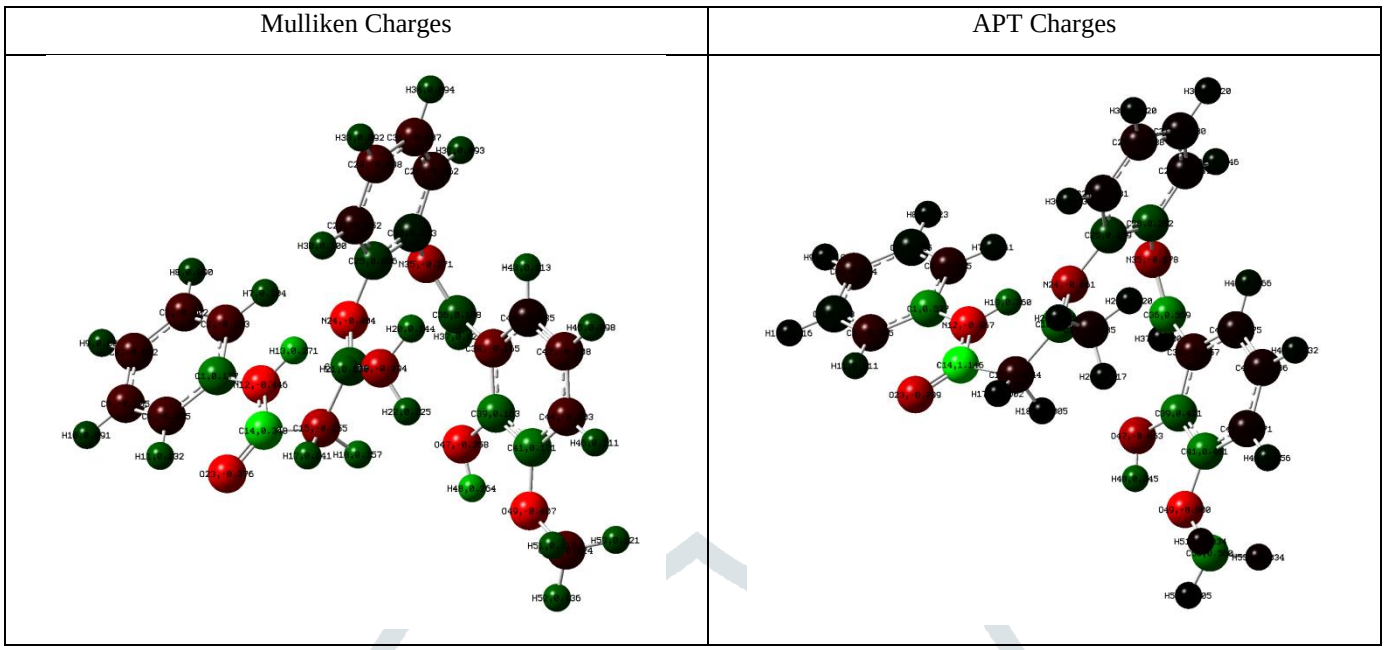

Fig. 3: Mulliken and APT charges of AAVA

Table 3: Computed electronic characters of AAVA

Electronegativity (c) (a.u)	0.1350
Hardness (h) (a.u))	0.0745
Softness (S) (a.u)	0.2979
Electrophilicity index (w) (a.u)	0.1223
ΔE_{gap} (LUMO-HOMO) (eV)	4.0532
Dipole moment (Debey)	8.17
Polarizability (α)	298.1266

III.3 Dipole moments

The dipole moment of the reported compound was computedwith B3LYP/6-311G(d,p) level of theory is given in Table 4 and it indicates bond polarities and charge densities in molecules. The dipolemoment value of AAVAis8.17D,which significantly showed that the AAVAis polarized and less active in nature [40].

III.4. Molecular Electrostatic Potential (MEP)

The molecular electro-static potential surface of the AAVA has been determined by B3LYP/6-311G(d,p) method to know the relative polarity of the molecules. The electrostatic potential contour map for positive and negative potentials of 'keto' form of AAVAis shown in Fig.4.The electron rich or negative charge of the MEP surface is shown in red colour, the blue region exposes the electron deficientor partially positive charge. The region around carbonyl oxygen atoms represents the most negative potential region (red). The hydrogen atoms attached to the end of methyl and methylene group possess the positive charge (blue). [38,39]

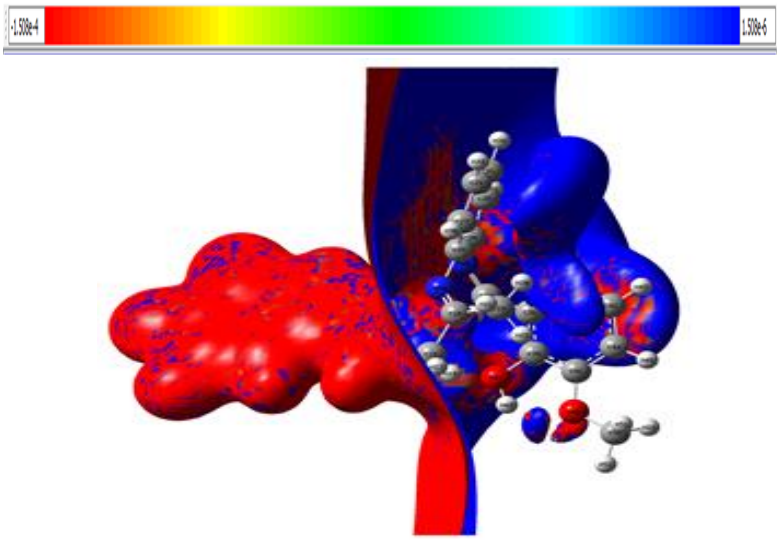

Fig. 4:ESP Contour plots of AAVA

III.5. Analysis of frontier molecular orbitals(FMO)

Frontier molecular orbital (FMOs) are highest occupied molecular orbital and lowest unoccupied molecular orbital. A molecular orbital describes the behavior of electrons in a molecule.Electrostatic potential of a molecule is a good tool to assess the molecules reactivity towards positively or negatively charged reactants [19]. The energies ofHOMO, LUMOand their orbital energygap are calculated by using B3LYP/6-311G(d,p) method.Thepictorial representation of the frontier molecular orbitals and theirrespective positive and negative regions are presented in Fig.5.The positive and negative surfaces areshown in red and greencolour, respectively. The electron cloud is mainly located on the anilide ring and is of π type, but in case of LUMO it is π* in nature, therefore, the HOMO–LUMO transition is π→π* in nature. The FMOs play crucial role in the optical and electrical properties of molecules. The energy gap between HOMO and LUMO helps to predict the chemical reactivity and kinetic stability of the molecule. A molecule with small energy gap has high chemical reactivity and low kinetic stability [36,37]. The energy gap value reveals thehigher chemical reactivity and lower kinetic stability. The energy gapof LUMO-HOMO is4.0532eV, which clearly indicates the charge transfer interface with in the molecule. The smaller energy gap between HOMO and LUMO facilitates molecule to be NLO active.

HOMO

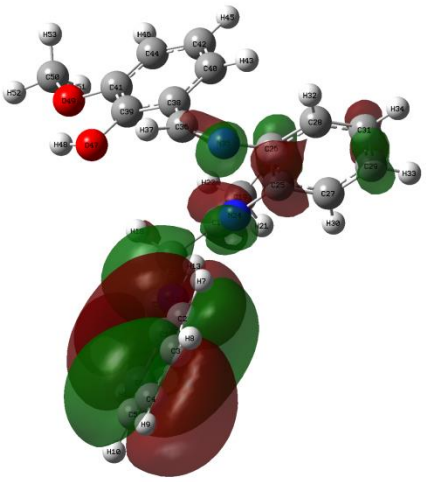

-0.20946

LUMO

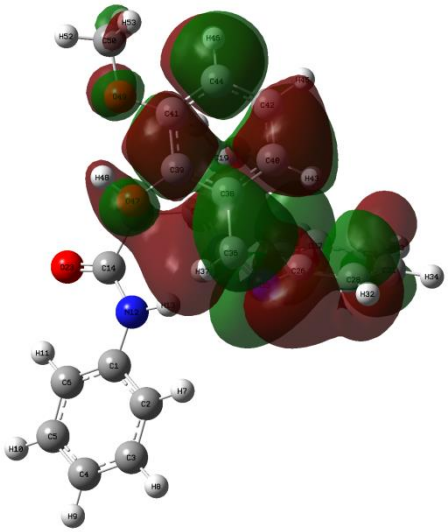

-0.06051

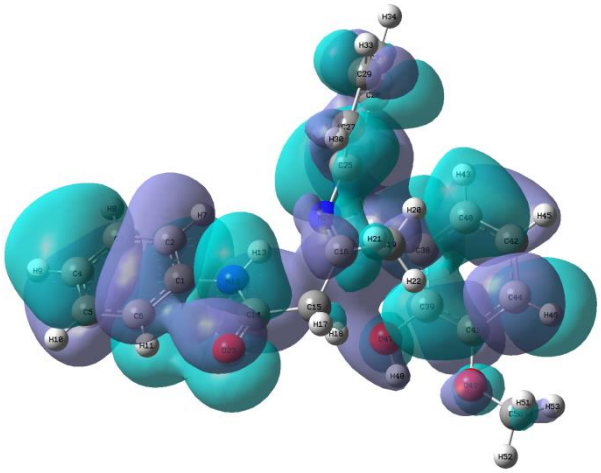

LUMO-HOMO=ΔE_{gap} **(eV) = 4.0532**

Fig. 5:HOMO-LUMO surfaces of AAVA

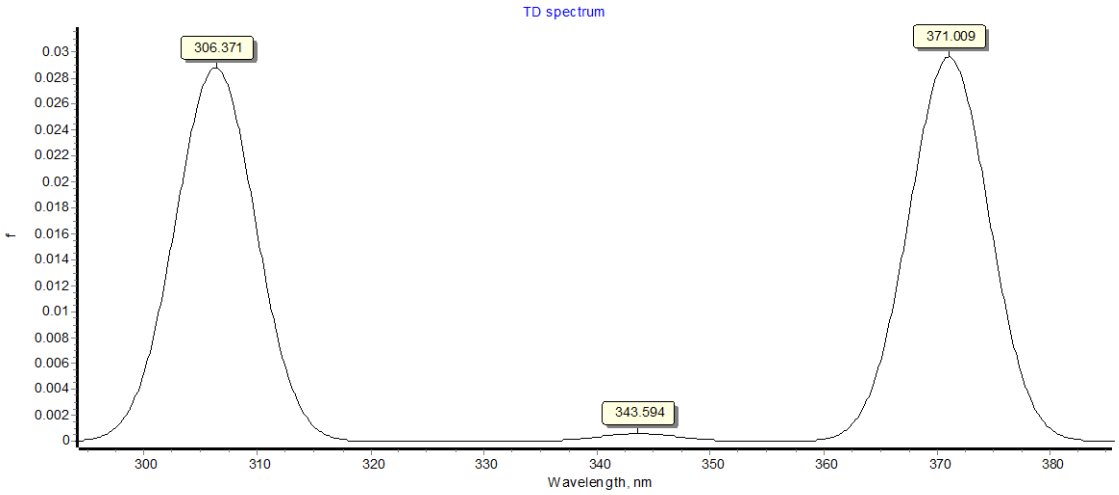

Fig. 6: UV-Visible Spectrum of AAVA

III.6. Electronic Transition

The electronic transitions of the AAVA has been explained based on time dependent density functional theory with B3LYP/6-311G(d,p) at gas phase using the optimized geometry of the ground state (Fig.6). AAVA-keto form gives intense peak at 317, 343 and 306 nm are assigned to π→π* and n→π* transitions of the conjugated anilideand diaminerings (Table 4). The most intense electronic transition occurs between the highest occupied molecular orbital to the lowest unoccupied molecular orbital, the energy gap is about E_{gap} = 4.0532eV (Fig.6 and Fig.7).

Table 4: UV-Vis (TD-DFT) Energy Excitation levels of AAVA

Absorption wavelength (nm)	Absorbance
371	0.0296
343	0.0006
306	0.0288

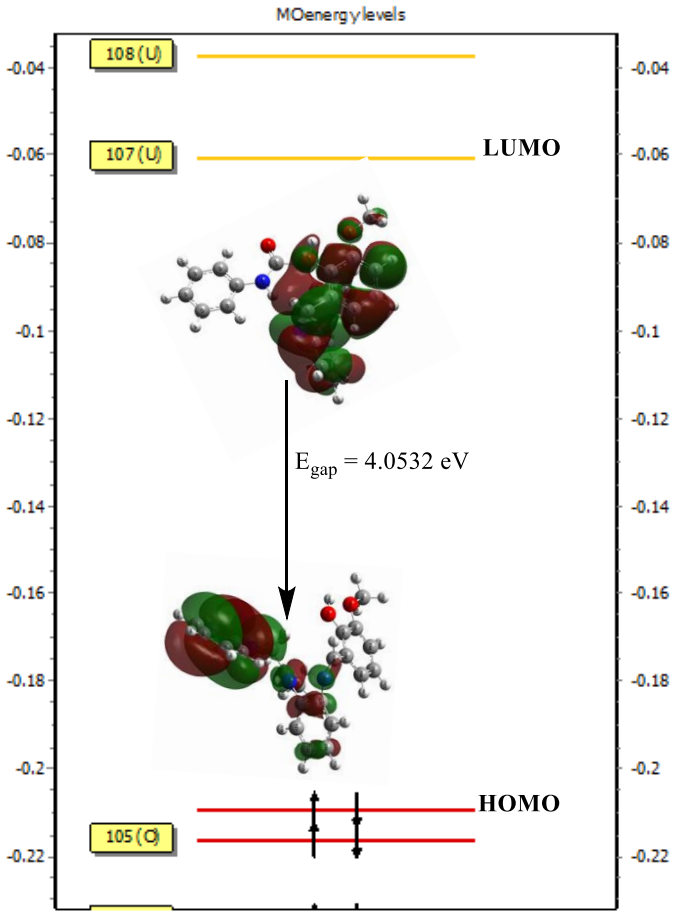

Fig. 8: Molecular Energy level diagram of AAVA

III.7. Computed Vibrational frequencies

IR frequencies with scaled values (Scaled with 0.958) are computed and is shown in Table 5 (Fig.8) with B3LYP/6-311G(d,p) level of theory. IR spectrum shows band at 1466, 14580, 1484 and 1434 cm^{-1} are attributed to methylene and methyl group of AAVA. Carbonyl group gives band at around 1755 cm^{-1} and the band at 3193cm^{-1} is assigned to N-H stretching. Carbon-Carbon stretching band of phenyl group is appeared in range of 1650-1200 cm^{-1} and the phenolic –OH is appearing at 3763cm^{-}. The bands at 3009 and 3079 $cm^{-1}$are due to the aromatic $–OCH_3$ and C-H stretching vibration respectively. C=N stretching appears at 1628 cm^{-1} and C-N stretching arises at 1257. The band observed at 1530 cm^{-1}iscorresponding to aromatic C=C stretching.All other vibrational bands of aromatic C-H stretching, aromatic C=C stretching and C=N stretching are 3074, 1530 and 1626 cm^{-1} respectively.

Table 5. Experimental and calculated IR intensities of AAVA using DFT with B3LYP/6-311G(d,p) in gas phase

IR Frequency	Frequency scaled with 0.958	IR Frequency	Frequency scaled with 0.958
524	502	963	923
530	507	976	935
543	520	976	935
555	531	977	936
556	533	1001	959
570	546	1010	968
588	564	1015	973
604	578	1050	1006
625	598	1053	1008
633	606	1062	1017
662	634	1100	1053
674	645	1104	1057
709	679	1110	1064
716	686	1124	1077
729	699	1172	1123
746	715	1179	1129
758	727	1181	1131
772	739	1185	1135
782	749	1193	1143

788	755	1202	1151
797	764	1206	1155
812	778	1209	1158
830	795	1220	1168
843	808	1243	1191
852	816	1248	1196
866	829	1254	1201
879	842	1257	1205
885	848	1280	1226
894	857	1289	1235
909	871	1299	1245
921	882	1310	1255
930	891	1315	1260
948	908	1342	1286
962	922	1356	1299
1359	1302	3012	2886
1397	1338	3028	2901
1404	1345	3074	2945
1434	1373	3079	2950
1446	1385	3100	2970
1473	1411	3104	2974

1478	1416	3142	3010
1478	1416	3142	3010
1480	1418	3157	3024
1484	1421	3164	3031
1491	1429	3166	3033
1497	1434	3174	3041
1503	1439	3175	3042
1510	1446	3182	3048
1513	1450	3185	3051
1530	1466	3187	3054
1596	1529	3193	3059
1600	1533	3204	3069
1626	1558	3212	3077
1628	1560	3241	3105
1644	1575	3383	3241
1650	1581	3763	3605
1652	1583		
1710	1638		
1723	1651		
1755	1681		
3009	2883		

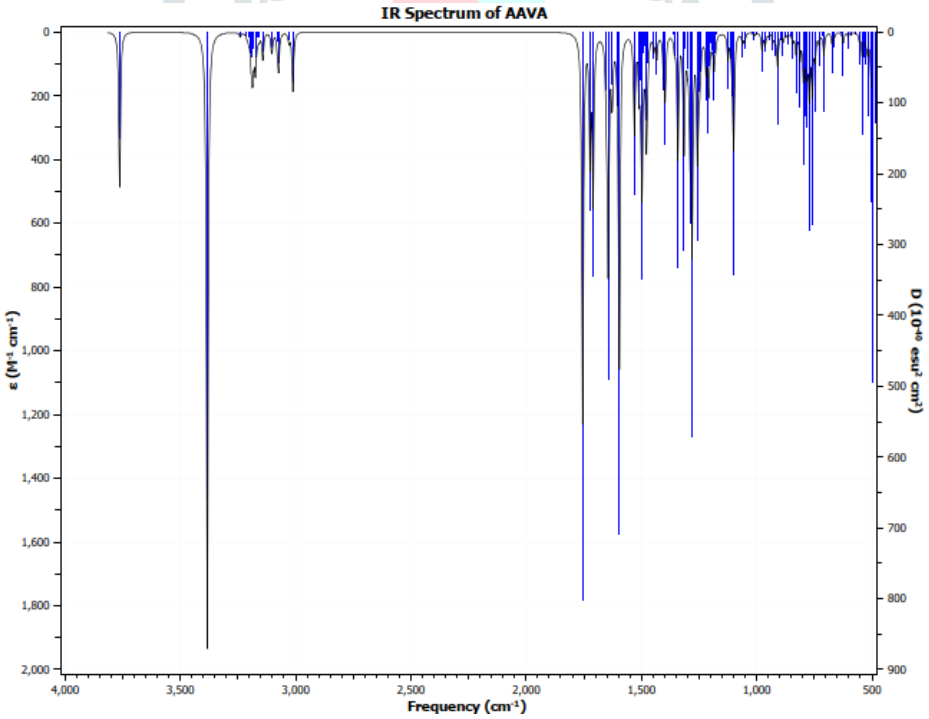

Fig. 8: IR Spectra of AAVA

III.8. NMR Chemical Shifts

The NMR techniques are used to predict presence of particular nuclei in a compound.It helps to elucidate the molecular structural information when the nucleus exposed to electromagnetic radiation in a strong magnetic field [40]. The geometry optimization of AAVA was performed at the gradient corrected density functional level of theory using the hybrid B3LYP method based on Becke's three parameters functional of DFT and gauge-including atomic orbital (GIAO) $^{13}C\{^{1}H\}$-NMR chemical shift calculations of the compound has been computedusing B3LYP/6-311G(d,p) basis set[38,39]. ^{1}H NMR (Fig.9) and ^{13}C-NMR (Fig. 10) chemical shifts of the compounds AAAP and ATAP with corresponding tautomeric forms are given in Table 6. Aromatic

carbons give signals in the range 100-150 ppm and the -I effect of nitrogen(N16) reduces the electron density of the carbon atom C1 thus NMR signal is observed in the downfield at 145.21 ppm. The acetyl methyl group carbon (C19) gives chemical shift at19.87 ppmand methyl carbon is observed at 48.31 ppm which reveals that the downfield is due to the influence of adjacent highly polar carbonyl group. Methyl carbon is shifted to downfield is due to electron withdrawing nature of carbonyl group. The carbonyl carbon appears at 174.49ppm [15].

Table 6: ^{1}H-NMR and ^{13}C-NMR shielding of AAVA

^{1}H-NMR		^{13}C-NMR	
Atoms	Shielding (ppm)	Atoms	Shielding (ppm)
13-H	10.38	16-C	174.49
37-H	9.01	14-C	164.61
11-H	8.84	36-C	162.27
32-H	7.38	39-C	152.65
34-H	7.30	41-C	151.21
10-H	7.25	26-C	150.77
8-H	7.18	1-C	145.21
33-H	6.99	25-C	138.79
9-H	6.91	5-C	132.38
7-H	6.80	3-C	131.33
43-H	6.64	31-C	129.37
30-H	6.47	38-C	126.87
45-H	6.44	28-C	126.51
46-H	6.42	40-C	125.66
48-H	5.37	29-C	125.28
52-H	4.04	4-C	125.24
51-H	3.60	27-C	124.02
53-H	3.52	6-C	121.81
18-H	3.14	42-C	120.94
17-H	2.70	2-C	120.21
20-H	1.48	44-C	111.18
21-H	1.39	50-C	54.76
22-H	0.45	15-C	48.31
		19-C	19.87

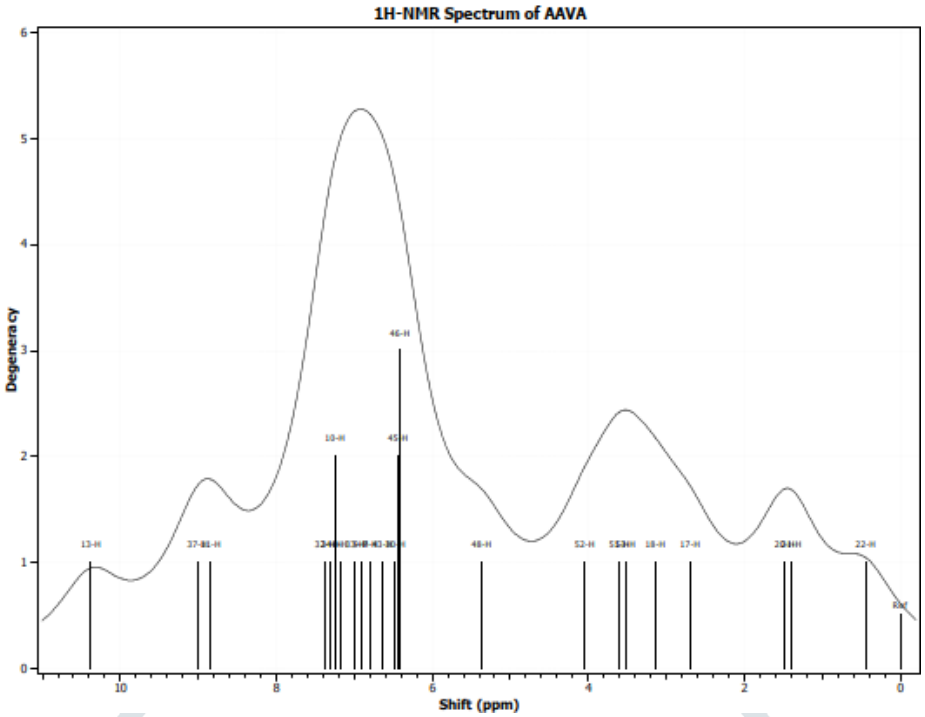

Fig. 9: ^{1}H-NMR Spectra of AAVA using DFT with B3LYP/6-311G(d,p) SCF GIAO Method

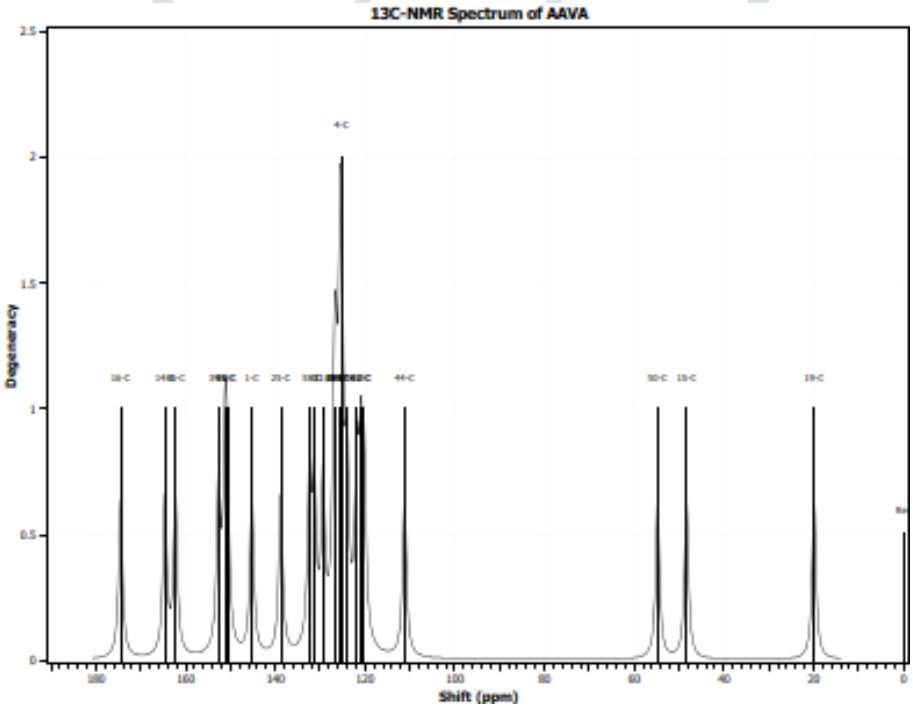

Fig. 101: ^{13}C-NMR Spectra of AAVAusing DFT with B3LYP/6-311G(d,p) SCF GIAO Method

The $–CH_2$- protons signal shifted to downfield than that of $–CH_3$ protons due to the adjacent electron withdrawing carbonyl group [15].AAVA spectrum shows set of peaks at 6.99 ppm to 7.30 ppm are attributed to protons in the aromatic ring. A peak appeared at 10.30 ppm is assigned to proton of nitrogen (N-H). Protons adjacent to nitrogen in the aromatic ring appear at 6.272 ppm and 6.51 ppm. Multiple peaks appear around 6.19 to 7.38 ppm is due to the presence of proton in the aromatic ring with hydroxide group. The presence of peak at 3.60 ppm is due to the phenolic $-OCH_3$.

III.9. Non-linear optical (NLO) properties

The NLO calculations have made an important contribution to the electronic polarization of molecule and structural properties relationship and the NLO response calculation was performed on the optimized geometry using B3LYP/6-311G(d,p) level of theory and the first static hyperpolarizability is a third rank tensor that can be described by a 3×3×3 matrix with 27 components of

the 3D matrix can be reduced to 10components due to the Kleinman symmetry [44-47], i.e., β_{xxx}, β_{xxy}, β_{xyy}, β_{yyy}, β_{xxz}, β_{xyz}, β_{yyz}, β_{xzz}, β_{yzz} and β_{zzz} respectively and the computed first static hyperpolarizability(β)values of these acetoacetanilidederivatives were calculated and converted to electrostatic units (esu) and represented in the Table 7. The calculated first static hyperpolarizability (β) tensors of AAVA isβ_{tot}= 1.7050 x 10^{-30}e.s.u.Hence, the title compoundwaspredicted to have larger NLO property[48,49].

Table 7:Computed second order hyperpolarizabilities of AAVA

β_{XXX}	β_{XYY}	β_{XZZ}	β_{YYY}	β_{YXX}	β_{YZZ}	β_{ZZZ}	β_{ZXX}	β_{ZYY}	β_{XYZ}	β_{TOT} **x 10^{-30}esu**
115.17	106.15	20.05	-50.15	-73.64	11.18	15.99	-15.91	-10.60	-13.2597	**2.303**

IV. CONCLUSIONS

In our attempt to elucidate the structural investigation on AAVA by the DFT calculations using B3LYP/6-311G (d,p) level of theory to evaluate the PES, vibrational frequencies (IR), electronic transition, TD-DFT and NMR shielding tensors (^{13}C and ^{1}H). Further, Mulliken Charges, APT charges, the energies of the frontier molecular orbitals (HOMO/LUMO) with molecular energy level diagram and electrostatic potential surface analysis were computed. In addition, an investigation of molecular first static hyperpolarizability (β_{tot}) was also calculated. The geometry optimization and dipole moment value shows that the compound is relatively polarized. The region around carbonyl oxygen atoms represents the most negative potential region (red) and the hydrogen atoms attached to the end of methyl and methylene group possess the positive charge (blue) in the molecular electro-static potential surface. The energy gap of LUMO-HOMO of AAVA is 4.0532eV, which clearly indicates the charge transfer interface with in the molecule. The energy gap reveals that the compound has higher chemical reactivity and lower kinetic stability. The narrow energy gap between HOMO and LUMO facilitates molecule to be NLO active.

Acknowledgements

The authors A. Manimaran and V.D. Nadhiya sincerely acknowledge the Management, Kongunadu Arts and Science College, Coimbatore-641 029, India for providing us with basic infrastructures to carry out this research.

Confilicts of Interest

Authors there is no conflicts of interests.

REFERENCES

[1] Deilami A.B., Salehi M., Amiri A., Arab A., New copper(II) and vanadium(IV) complexes based on allylamine-derived Schiff base ligand; synthesis, crystal structure, electrochemical properties and DFT calculations, *Journal of Molecular Structure*, **1181**: 190-196 (2019).

[2] Haque Faizi M.S., Haque A., Dege M., Degec N., Malysheva M.L., Crystal structure and DFT study of (E)-2,6-di-tertbutyl-4-{[2-(pyridin-2-yl)hydrazin-1-ylidene)methyl} Phenol, *Acta Cryst.* **E73**: 1449–1452 (2017).

[3] Saleem H., Subashchandrabose S., Ramesh Babu N., Syed Ali Padusha M., Vibrational spectroscopy investigation and density functional theory calculations on (E)-N′-(4-methoxybenzylidene) benzohydrazide, *Spectrochimica Acta Part A: Molecular and Biomolecular Spectroscopy*, **143**: 230–241(2015).

[4] Annaraj B., Pan S., Neelakantan M.A., Chattaraj P.K., DFT study on the ground state and excited state intramolecular proton transfer of propargyl arm containing Schiff bases in solution and gas phases, *Computational and Theoretical Chemistry*, **1028**:19–26(2014).

[5] Elmacı G., Duyar H., Aydıner B., Yahaya I., Seferoğlu N., Şahin E., PınarÇelik S., Açık L., Seferoğlu Z., Novel benzildihydrazone based Schiff bases: Syntheses, characterization, thermal properties, theoretical DFT calculations and biological activity studies, *J. Mol. Struct.*, **1184**:271-280 (2019).

[6] Curottoa V.F., Echeverría G.A., Piro O.E., Pis-Diez R., González-Baró A.C., Synthesis and characterization of a series of isoniazid hydrazones. Spectroscopic and theoretical study, *J. Mol. Struct.*, **1133**: 436-447 (2017).

[7] Abdel-Rahman L.H., Ismail N.M., Ismael M., Abu-Dief A.M., Ahmed E.A.H., Synthesis, characterization, DFT calculations and biological studies of Mn(II), Fe(II), Co(II) and Cd(II) complexes based on a tetradentate ONNO donor Schiff base ligand, *J. Mol. Struct.*, **1134** : 851-862 (2017).

[8] Temel E., Alasalvar C., Gökçe H., Güder A., Albayrak C., Alpaslan Y.B., Alpaslan G., Dilek N., DFT calculations, spectroscopy and antioxidant activity studies on (E)-2-nitro-4-[(phenylimino)methyl]phenol, *Spectrochimica Acta Part A: Molecular and Biomolecular Spectroscopy*,**136**: 534–546 (2015).

[9] Kew-YuChen, Jiun-WeiHu, Excited-state charge coupled proton transfer reaction in dipole-functionalized salicylideneaniline, *Journal of Luminescence*,**159**: 171–177 (2015).

[10] Odabas M., Albayrak C., Kosarb B., Büyükgüngör O., Synthesis, spectroscopic characterizations and quantum chemical computational studies of (Z)-4-[(E)-p-tolyldiazenyl]-6-[(2-hydroxyphenylamino)methylene]-2-methoxycyclohexa-2,4-dienone, *Spectrochimica Acta Part A* , **92**: 357– 364 (2012).

[11] Ravikumar C., Hubert Joe I., Sajan D., Vibrational contributions to the second-order nonlinear optical properties of p-conjugated structure acetoacetanilide, *Chemical Physics*, **369**: 1–7 (2010).

[12] Demircioglu Z., Albayrak C., Büyükgüngör O., The spectroscopic (FT-IR, UV–vis), Fukui function, NLO, NBO, NPA and tautomerism effect analysis of (E)-2-[(2-hydroxy-6-methoxybenzylidene)amino]benzonitrile, *Spectrochimica Acta Part A: Molecular and Biomolecular Spectroscopy*, **139**: 539–548 (2015).

[13] Finkel T., Radical medicine: treating ageing to cure disease, *Nat. Rev. Mol. Cell Biol.*, **6:** 971-976 (2005).

[14] Padma Priya N., Arunachalam S., Manimaran A., Muthupriya D., Jayabalakrishnan C., Mononuclear Ru(III) Schiff base complexes: Synthesis, spectral, redox, catalytic and biological activity studies, SpectrochimicaActa Part A, **72**:670–676 (2009).

[15] Arjunan V., Kalaivani M., Senthilkumari S., Mohan S., Vibrational, NMR and quantum chemical investigations of acetoacetanilde, 2-chloroacetoacetanilide and 2-methylacetoacetanilide, *SpectrochimicaActa Part A: Molecular and Biomolecular Spectroscopy*, **115**:154–174 (2013).

[16] Abdalrazaq Eid A., Al-Ramadane Omar M., Al-NumaKhansa S., Synthesis and Characterization of Dinuclear Metal Complexes Stabilized by Tetradentate Schiff Base Ligands**,** *American Journal of Applied Sciences*, **7 (5)**:628-633 (2010).

[17] De Geest D.J., Noble A., Moubaraki B., Murray K.S., Larsen D.S., Brooker S., Dicopper(II) complexes of a new pyrazolate-containing Schiff-basemacrocycle and related acyclic ligand, *Dalton Trans*, **28:**467-475 (2007).

[18] Witzeman J.S., Nottingham W.D., Transacetoacetylation with tert-butyl acetoacetate: synthetic applications, *J. Org. Chem*., **56**:1713–1718 (1991).

[19] Alasalvar C., Soylu M. S., Güder A., Albayrak Ç. D., Apaydın G., Dilek N., Crystal structure, DFT and HF calculations and radical scavenging activities of (E)-4,6-dibromo-3-methoxy-2-[(3-methoxyphenylimino)methyl]phenol, *SpectrochimicaActa Part A: Molecular and Biomolecular Spectroscopy*, **125**: 319–327 (2014).

[20] Pouralimardan O., Chamayou A.C., Janiak C., Hosseini-Monfared H., Hydrazone Schiff base-manganese (II) complexes: Synthesis, crystal structure and catalytic reactivity, *Inorg. Chim. Acta*, **360**:1599–1608 (2007).

[21] PandeyA.K, Shukla D.K, Singh V, Narayan V. Structural, IR spectra NBO, TDDFT, AIM calculation, biological activity and docking property of [1,2,4]-triazolo[3,4-*b*][1,3,4] thiadiazole, *Egyptian Journal of Basic and Applied Science,* 5(4): 280-288 (2018).

[22] Kohn W., Nobel Lecture:Electronic structure of matter-wave functions and density functional, *Rev. Mod. Phys*., **71:**1253-1266 (1999).

[23] Becke A. D., Density-functional exchange-energy approximation with correct asymptotic behavior, *Phys. Rev A*, **38:**3098 (1988).

[24] Lee C., Yang W., Parr R.G., Development of the Colle-Salvetti correlation-energy formula into a functional of the electron density, *Phys. Rev. B*, **37:**785 (1988).

[25] Frisch M. J., Pople J. A., Binkley J. S., Self-consistent molecular orbital methods 25. Supplementary functions for Gaussian basis sets, *J. Chem. Phys*., **80**:3265-3269 (1984).

[26] Hehre W. J., Radom L., Schleyer P. V. R., Pople J. A., "Ab initio Molecular Orbital Theory", John Wiley, New- York (1986).

[27] Frisch M.J., Trucks G.W., Schlegel H.B., Scuseria G.E., Robb M.A., Cheeseman J.R., Scalmani G., Barone V., Mennucci B., Petersson G.A., Nakatsuji H., Caricato M., Li X., Hratchian H.P., Izmaylov A.F., Bloino J., Zheng G., Sonnenberg J.L., Hada M., Ehara M., Toyota K., Fukuda R., Hasegawa J., Ishida M., Nakajima T., Honda Y., Kitao O., Nakai H., Vreven T., Montgomery J.A., Peralta Jr., J.E., Ogliaro F., Bearpark M., Heyd J.J., Brothers E., Kudin K.N., Staroverov V.N., Kobayashi R., Normand J., Raghavachari K., Rendell A., Burant J.C., Iyengar S.S., Tomasi J., CossiM.,Rega N., Millam J.M., Klene M., Knox J.E., Cross J.B., Bakken V., Adamo C., Jaramillo J., Gomperts R., Stratmann R.E., Yazyev O., Austin A.J., Cammi R., Pomelli C., Ochterski J.W., Martin R.L., Morokuma K., Zakrzewski V.G., Voth G.A., Salvador P., Dannenberg J.J., Dapprich S., Daniels A.D., Farkas O., Foresman J.B., Ortiz J.V., Cioslowski J., Fox D.J., "Gaussian 09", Inc., Wallingford, CT (2009).

[28] Ditchfield R., Self-consistent perturbation theory of diamagnetism: I. A gauge-invariant LCAO method for N.M.R. chemical shifts, *Mol. Phys.*, **27:**789-807 (1974).

[29] Fukui H., Miura K.,Shinbori H., Calculation of NMR chemical shifts. VI. Gauge invariant and Hermitian condition, *The Journal of Chemical Physics*, **83**:907-908 (1985).

[30] Wolinski K. , Hinton J. F., Pulay P., Efficient implementation of the gauge-independent atomic orbital method for NMR chemical shift calculations, *J. Am. Chem. Soc.*, **112:**8251–8260 (1990).

[31] Häser M., Ahlrichs R., Baron H. P., Weiss P., Horn H. , Direct computation of second-order SCF properties of large molecules on workstation computers with an application to large carbon clusters, *Theor. Chem. Acc.*, **83:**455 (1992).

[32] Chidangil S., Shukla M.K., Mishra P.C., A molecular electrostatic potential mapping study of some fluoroquinolone anti-bacterial agents, *J. Mol. Model.*, **4**:250–258 (1998).

[33] Murray J.S., Sen K., "Molecular Electrostatic Potentials, Concepts and Applications", Elsevier, Amsterdam (1996).

[34] Krishnakumar V., Keresztury G., Sundius T., Ramasamy R., Simulation of IR and Raman spectra based on scaled DFT force fields: A case study of 2-(methylthio)benzonitrile, with emphasis on band assignment,*J. Mol. Struct.*, **702**:9–21 (2004).

[35] Dennington II Roy D., Keith Todd A., Millam John M., "Gauss View", Version 6.0.16, Semichem, Inc. (2000-2016).

[36] Wang Y., Saebar S., Pittman Jr C.U., The structure of aniline by ab initio studies, *J. Mol. Struct.(Theochem)*, **281**:91–98 (1993).

[37] Şahin Ö., ÖzmenÖzdemir Ü., Seferoğlu N., KaragözGenc Z., Kaya K., Aydıner B., Tekin S., Seferoğlu Z., New platinum (II) and palladium (II) complexes of coumarin-thiazole Schiff base with a fluorescent chemosensor properties: Synthesis, spectroscopic characterization, X-ray structure determination, in vitro anticancer activity on various human carcinoma cell lines and computational studies, *Journal of Photochemistry & Photobiology, B: Biology*, **178**:428–439 (2018).

[38] Demircioglu Z., AlbayrakKastas C., Buyukguugor O., The spectroscopic (FT-IR, UV–vis), Fukui function, NLO, NBO, NPA and tautomerism effect analysis of (E)-2-[(2-hydroxy-6-methoxybenzylidene)amino]benzonitrile, *SpectrochimicaActa Part A: Molecular and Biomolecular Spectroscopy*, **139**:539–548 (2015).

[39] Fleming I., "Frontier Orbitals and Organic Chemical Reactions", Wiley, London (1976).

[40] Reed A.E., Weinhold F., Natural localized molecular orbitals, *J. Chem. Phys.*, **83**:1736–1740 (1985).

[41] Reed A.E., Weinstock R.B., Weinhold F., Natural population analysis, *J. Chem. Phys.*, **83**:735–746 (1985).

[42] Dani V.R., "Organic Spectroscopy", Tata McGraw Hill, New Delhi (1995).

[43] Von Schleyer P., Maerker C. , Dransfield A., Jiao H., Van EikemaHommes N. J. R., Nucleus-Independent Chemical Shifts: A Simple and Efficient Aromaticity Probe, *J. Am. Chem. Soc.*, **118**:6317 (1996).

[44] Parr R.G., Pearson R.G., Absolute hardness: companion parameter to absolute electronegativity, *J. Am. Chem. Soc.*, **105**:7512-7516 (1983).

[45] Parr R.G., Szentpaly L.V., Liu S., Electrophilicity Index, *J. Am. Chem. Soc.*, **121**:1922-1924 (1999).

[46] WrightJ.S., CarpenterD.J., McKayD.J., IngoldK.U., Theoretical Calculation of Substituent Effects on the O−H Bond Strength of Phenolic Antioxidants Related to Vitamin E, *J. Am. Chem. Soc.*,**119**:4245-4252(1997).

[47] MiertusS., ScroccoE., TomasiJ., Electrostatic interaction of a solute with a continuum. A direct utilizaion of AB initio molecular potentials for the prevision of solvent effects,*Chem. Phys.*,**55**:117-129(1981).

[48] MiertusS., TomasiJ., Approximate evaluations of the electrostatic free energy and internal energy changes in solution processes,*Chem. Phys.*,**65:**239-245(1982).

[49] KleinmanD.A., Nonlinear Dielectric Polarization in Optical Media,*Phys. Rev.*,**126:**1977-1979(1962).